AGU100 ADVANCING EARTH AND SPACE SCIENCE

Geophysical Research Letters

RESEARCH LETTER
10.1029/2018GL077826

Key Points:
- The Northern winter stratospheric response shifts from an easterly to a westerly wind change between two global warming periods of 2 K
- The nonlinear stratospheric response can be related to differences in the November Arctic amplification and sea ice changes
- The nonlinear stratospheric response appears to couple back to the surface climate response over the North Atlantic-European region

Supporting Information:
- Supporting Information S1

Correspondence to:
E. Manzini,
elisa.manzini@mpimet.mpg.de

Citation:
Manzini, E., Karpechko, A. Y., & Kornblueh, L. (2018). Nonlinear response of the stratosphere and the North Atlantic-European climate to global warming. *Geophysical Research Letters*, *45*, 4255–4263. https://doi.org/10.1029/2018GL077826

Received 7 MAR 2018
Accepted 8 APR 2018
Accepted article online 19 APR 2018
Published online 4 MAY 2018

Nonlinear Response of the Stratosphere and the North Atlantic-European Climate to Global Warming

E. Manzini[1], A. Yu. Karpechko[2], and L. Kornblueh[1]

[1]Max-Planck-Institut für Meteorologie, Hamburg, Germany, [2]Finnish Meteorological Institute, Helsinki, Finland

Abstract The response of the northern winter atmospheric circulation for two consecutive global warming periods of 2 K is examined in a grand ensemble (68 members) of idealized CO_2 increase experiments performed with the same climate model. The comparison of the atmospheric responses for the two periods shows remarkable differences, indicating the nonlinearity of the response. The nonlinear signature of the atmospheric and surface responses is reminiscent of the positive phase of the annular mode of variability. The stratospheric vortex response shifts from an easterly wind change for the first 2 K to a westerly wind change for the second 2 K. The North Atlantic storm track shifts poleward only in the second period. A weaker November Arctic amplification during the second period suggests that differences in Arctic sea ice changes can act to trigger the atmospheric nonlinear response. Stratosphere-troposphere coupling thereafter can provide for the persistence of this nonlinearity throughout the winter.

Plain Language Summary The effects of global warming are experienced in terms of changes in meteorological phenomena of the Earth's atmosphere, such as the storms that reach Europe, from their region of origin in the western North Atlantic. In this study, we analyzed a large ensemble of numerical experiments for the prediction of the atmospheric response to an idealized scenario of global warming. We compare changes for an initial 2 K warming with those of a follow-up 2-K warming. Of relevance to climate change in Europe, we found that changes in the preferred locations of the North Atlantic storms for the second 2 K of global warming cannot be predicted from their respective changes to the first 2 K of global warming. This result signifies that the atmospheric response does not scale with global warming.

1. Introduction

The response of the stratosphere to global warming is of interest to regional climate, because the stratospheric vortex strength has been shown to be one of the large-scale circulation drivers of surface changes for the Northern Atlantic-European region (Karpechko & Manzini, 2012; Manzini et al., 2014; Scaife et al., 2012; Zappa & Shepherd, 2017). Studies employing future projections of the stratospheric polar vortex have been so far focusing on contrasting multiyear or equilibrated mean changes, to facilitate the emergence of signals from internal dynamical variability.

The questions of how the stratospheric vortex and the transient climate responses may change for consecutive periods of equal global warming have not been addressed so far, because of the high internal variability of the stratospheric vortex and of the atmospheric flow in general. With the availability of large ensembles of idealized scenario experiments carried out with the same model, we can now address such questions. The use of the same model allows for the investigation of the transient (not equilibrated) mean climate change at a specific level of global warming, with the transient mean climate obtained by taking the ensemble mean of a large number of experiments, resulting in a time series with strongly reduced internal variability.

Here we make use of one such large ensemble to ask if circulation changes are linear with increasing global warming and if patterns of changes scale with global warming. Specifically, we examine how the stratospheric vortex and related aspects of transient climate change may differ for two consecutive periods of 2 K of global warming. A weakening of the stratospheric vortex (Manzini et al., 2014) and an increase in planetary wave driving have been related to increased sea surface temperatures and the strengthening of the zonal winds in the subtropics, near the tropopause (Karpechko & Manzini, 2017). However, also Arctic sea ice loss can increase the planetary wave driving (Hoshi et al., 2017; Kim et al., 2014; Nakamura et al., 2016; Sun et al., 2015). Once the sea ice is melted, there will no longer be a change in this source of planetary waves and consequently the increase in total planetary wave driving could be reduced. In addition, there can be competing effects. For instance, according to Hurwitz et al. (2012), warming of the North Pacific is related to a strong stratospheric polar vortex via a reduction of wave activity due to a weakening of the Aleutian low. Also, the atmospheric climatological basic state may affect the response (Sigmond & Scinocca, 2010). By examining the atmospheric circulation changes for two consecutive periods of 2 K of global warming, we aim to identify which drivers of stratospheric change may be linear or not, and in so doing search for evidence of the role of Arctic sea ice loss in leading to nonlinear responses.

2. Methods

2.1. Grand Ensemble

The large ensemble available to us consists of 68 idealized scenario experiments performed with the Max Planck Institute Earth System Model at Low Resolution (MPI-ESM-LR, Giorgetta et al., 2013), and is hereafter named "grand ensemble." The idealized scenario experiment follows the Coupled Model Intercomparison Project phase 5 (CMIP5) protocol (Taylor et al., 2012) of the 1pcCO_2 experiment, with a prescribed atmospheric CO_2 concentration increasing by 1% per year, while aerosols, other well mixed greenhouse gases, and ozone are equal for each year. Each experiment is 156-year long, to include CO_2 quadrupling (which occurs at year 140). The ensemble members are initialized from different years of a 2000 years long preindustrial control simulation performed with the same model. The analysis is restricted to monthly means, given that daily data are not available.

2.2. Analysis Design

In the stratosphere, internal dynamical variability is generally high. Therefore, variations in the monthly time series are reduced, by applying month by month a 15-year running mean by calendar month. The length of this averaging period, however, does not impact our conclusions. The 156-year time series is therefore reduced to a 142-year time series (at the start and end of the series 7 years are lost due to the running mean). Hereafter the year numbering refers to the 142 smoothed time series.

The first 2 K of global warming (diagnosed by the annual global mean temperature at 850 hPa) occurs at year 73, and the second at year 129. The second 2 K of warming (i.e., a total warming of 4 K) is therefore reached slightly faster (56 years instead of 73 years), because of a nonlinearity in the thermodynamical response related to the lapse rate water vapor feedback, a nonlinearity which is relatively small for small CO_2 perturbations (Giorgetta et al., 2013; Meraner et al., 2013), and the committed warming due to the ocean temperature imbalance, given that we are analyzing transient experiments.

To contrast the circulation changes for the two consecutive periods of global warming, we compute the following 10-year averages:

1. Initial state climate (average over years 1–10, the first decade);
2. Climate at 2 K of global warming (average over years 73–82, the second decade);
3. Climate at 4 K of global warming (average over years 129–138, the third decade).

The difference between the second and first decades (hereafter 2K1) provides information on the circulation changes for the first 2 K of global warming, and the difference between the third and the second decades (2K2) on the changes for the second 2 K. The degree of linearity between the changes for the two consecutive periods of global warming is obtained by differencing the 2K2 response and the 2K1 response (2K2 − 2K1). For a linear response 2K2 − 2K1 must be close to zero.

The 2K1 and 2K2 responses and their difference are computed by member and for the ensemble mean, for a number of selected meteorological monthly mean variables. The significance of ensemble mean differences between the decades is calculated by a two-sample Student's t test, given the two sample distributions of the 68 decadal means (by member), at each grid point. For the 2K2 − 2K1 difference, which involves four sample distributions, we followed the variant of the Student's t test described in Karpechko and Manzini (2012). Significance is marked for $p < 0.05$, where p is the probability of incorrect rejection of null hypothesis.

3. Stratospheric and Surface Responses

The Northern Hemispheric changes are diagnosed by latitude-pressure sections of the zonal mean zonal wind and maps of the near-surface zonal wind and the pressure at sea level (PSL). January is shown, but comparable results are found for December and February. Poleward of 60°N, the stratospheric responses to the

10.1029/2018GL077826

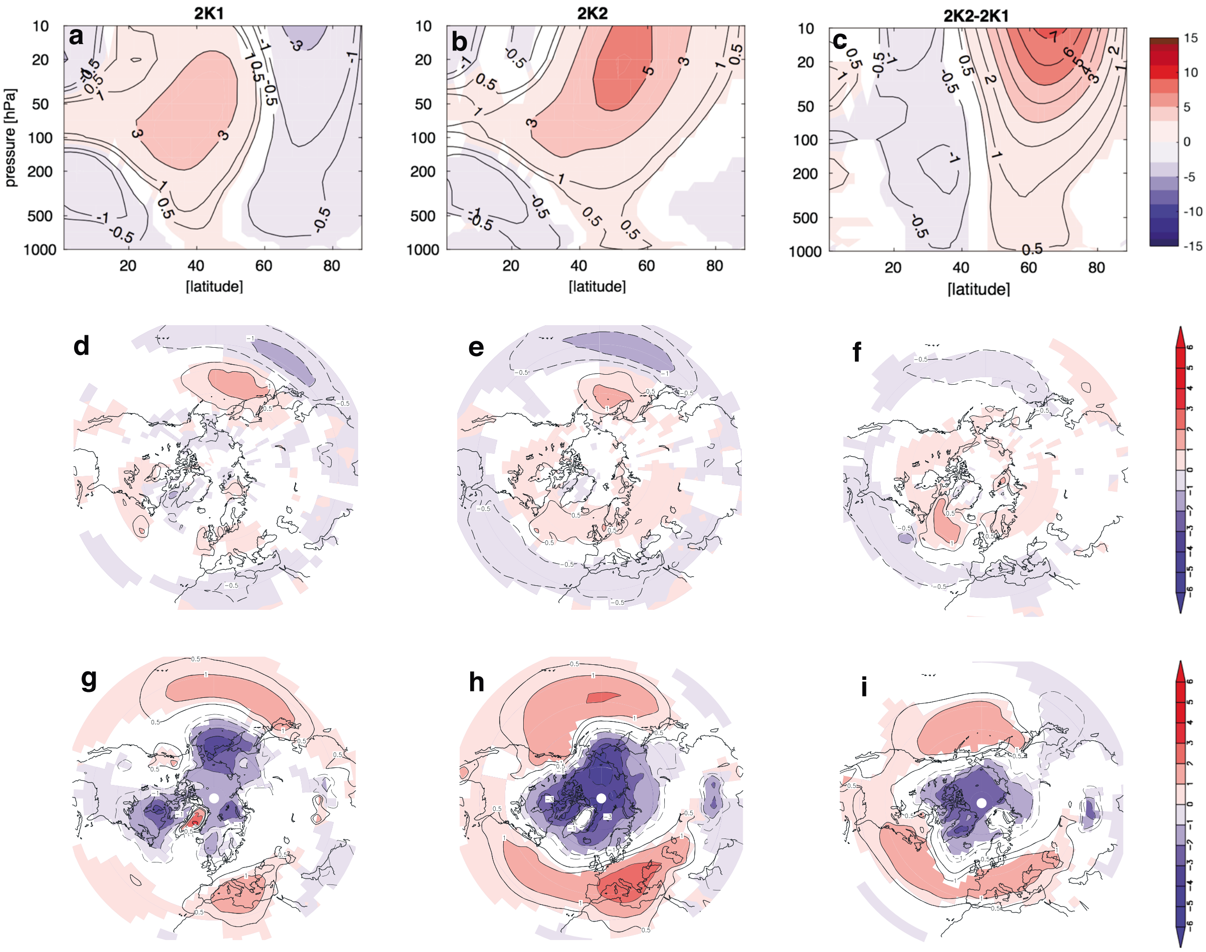

Figure 1. January response of zonal mean zonal wind (m/s) to (a) the first and (b) the second 2 K of global warming and (c) their difference. (d–f) Same as (a)–(c) but shown is near-surface (10 m) zonal wind (m/s). (g–i) Same as (a)–(c) but shown is pressure at sea level (hPa). Contours: (a, b) ±0.5, ±1 and then each 2 m/s; (c) ±0.5, ±1 and then each 1 m/s; (d, f) ±0.5, ±1 and then each 1 m/s; (g–i) ±0.5, ±1 and then each 1 hPa. Colored areas indicate significance with $p < 0.05$.

first and second 2 K of global warming are remarkably different (Figures 1a and 1b). The high-latitude stratospheric zonal mean zonal wind shifts from an easterly to a westerly change from the first to the second 2 K of warming. The nonlinear signature is characterized by stronger zonal winds poleward of ~50°N and weaker winds to the south, throughout the troposphere and stratosphere (Figure 1c). At high latitudes, the zonal mean zonal wind response is highly nonlinear in the stratosphere (~7 m/s of difference between the responses at 10 hPa). The nonlinearity continues to be significant throughout the troposphere. At the surface, the nonlinearity has a magnitude (~0.5 m/s) comparable to (or even larger than) the near-surface climate change signal itself. Equatorward of 50°N, the reduction of the strengthening of the subtropical tropospheric jet appears to be linked, likely through eddy momentum fluxes, to the high-latitude changes, rather than driven by tropical warming. The tropical tropospheric temperature response is indeed linear (supporting information Figure S1). In the stratosphere, the 2K2 period is slightly warmer, because the CO_2 change in 2K2 is slightly less than in 2K1 (2K2 includes less years). However, this radiatively driven change cannot explain the 2K2 − 2K1 polar cooling (Figure S1) and vortex strengthening. Note that the 2K2 stratospheric vortex strengthening is smaller in magnitude than the 2K1 weakening. As a result, the response at 4 K (Figure S2) shows a high-latitude easterly wind change, in agreement the most typical mean response (Karpechko & Manzini, 2017; Manzini et al., 2014).

Remarkable regional differences emerge from the inspections of the tropospheric maps. While over the North Pacific sector there is a comparable poleward shift of the near-surface zonal wind for both 2K1 and 2K2, indicating a mostly linear response, over the North Atlantic and Europe, a pronounced poleward shift of the jet stream occurs only for 2K2 (Figures 1d–1f). The North Atlantic storm track, which drives the near-surface zonal winds, appears therefore to change very little for the first 2 K of global warming. Consistently, a seesaw PSL change over the North Atlantic, corresponding to the positive phase of the North Atlantic Oscillation, occurs only during the second period (Figures 1g–1i; see also Figure S2 for the response at 4 K).

The quasi-zonally symmetric nonlinear signature in PSL is consistent with the zonal mean stratospheric nonlinear signature. The nonlinear signature in the circulation response is indeed reminiscent of the northern annular mode of variability, specifically of its positive phase (Thompson & Wallace, 2000). Given such a large-scale and vertically coherent nonlinear response in atmospheric circulation, identifying the sources of the nonlinearity is of extreme interest.

Next, we therefore examine changes in near-surface temperature, as a proxy for Arctic amplification (hereafter AA) and ocean circulation changes, and changes in quasi-stationary meridional eddy heat flux (hereafter SHF), to estimate changes in stratospheric wave forcing. Sea ice changes and AA are intimately connected. We examine nonlinearities in AA instead of the sea ice changes, because it is at the time when AA peaks (or later) that the atmospheric circulation is impacted (Sun et al., 2015). A complete investigation of the stratospheric wave forcing requires diagnosing the total eddy heat flux (or the Eliassen-Palm flux) including the transient component. However, only monthly mean output has been saved from the grand ensemble; hence, a complete analysis is not possible. McLandress and Shepherd (2009) and Karpechko and Manzini (2017) have shown that quasi-stationary planetary waves are an important component of the stratospheric response. Therefore, it is worth to evaluate the behavior of the SHF and ask if its response can shed light on the difference in the stratospheric response between the two periods.

4. Potential Drivers of the Nonlinear Circulation Response

Figures 2a–2d shows the October to April ensemble mean evolution of the nonlinear signature (the 2K2 − 2K1 difference) for AA and indicators of atmospheric changes. These are the SHF (zonal mean of the product of monthly mean eddy air temperature and meridional wind, where "eddy" indicates the departure from the respective zonal mean), the high-latitude zonal mean zonal wind in the stratosphere and the northern annular mode (hereafter NAM) PSL index. For definitions see the caption of Figure 2. October to April is shown, to focus on the northern winter and because nonlinearity is small during the rest of the year.

There is a marked reduction (~1 K) in November AA (Figure 2a), consistent with the fact that during the second period there is less sea ice to melt and that, specifically, the Barents-Kara (hereafter BK) and other Arctic marginal seas are ice free at the beginning of 2K2 (Figure S3). The AA reduction in November is about 25%, while in the annual mean, the reduction in AA is only about 10%, and AA continues unabated throughout the whole experiment (not shown).

The nonlinearity in lower stratospheric SHF (Figure 2b, 100 hPa) signifies not only a reduction of the increase of quasi-stationary wave activity, given that the flux is increased for 2K1 (Figure 3a, January), but also a net reduction (high-latitude negative change, Figure 3b). However, we do not know if there is a negative change of the total wave activity for 2K2, because we do not have daily data. However, the point of relevance is that at least a part of the total increase of the wave activity due to global warming is reduced, consistent with a decrease in the change of a wave forcing factor, namely, the factor associated with sea ice changes (manifested in the AA reduction and possibly also in the slight negative tropospheric SHF nonlinearity, Figure 2b, 500 hPa). This relationship between wave forcing and sea ice changes is consistent with the sensitivity to changes in autumn sea ice found in the experiments of Sun et al. (2015), and in analysis of the stratospheric response to recent sea ice changes (Hoshi et al., 2017; Nakamura et al., 2016), with a reversed sign, given that we are dealing with a reduction in sea ice changes, by contrasting the second to the first period of 2 K of global warming.

While the largest AA nonlinearity is limited to autumn, the nonlinearity in the atmospheric changes increases from October to January and/or February (Figures 2b–2d). The negative difference in the changes in stratospheric SHF (substantial in December and January, Figure 2b) is consistent with the strengthening of the stratospheric vortex (maximum in January, Figure 2c). The NAM nonlinearity shows an intensification of the positive phase throughout the winter (~2 hPa, Figure 2d). The persistence of the NAM nonlinearity till

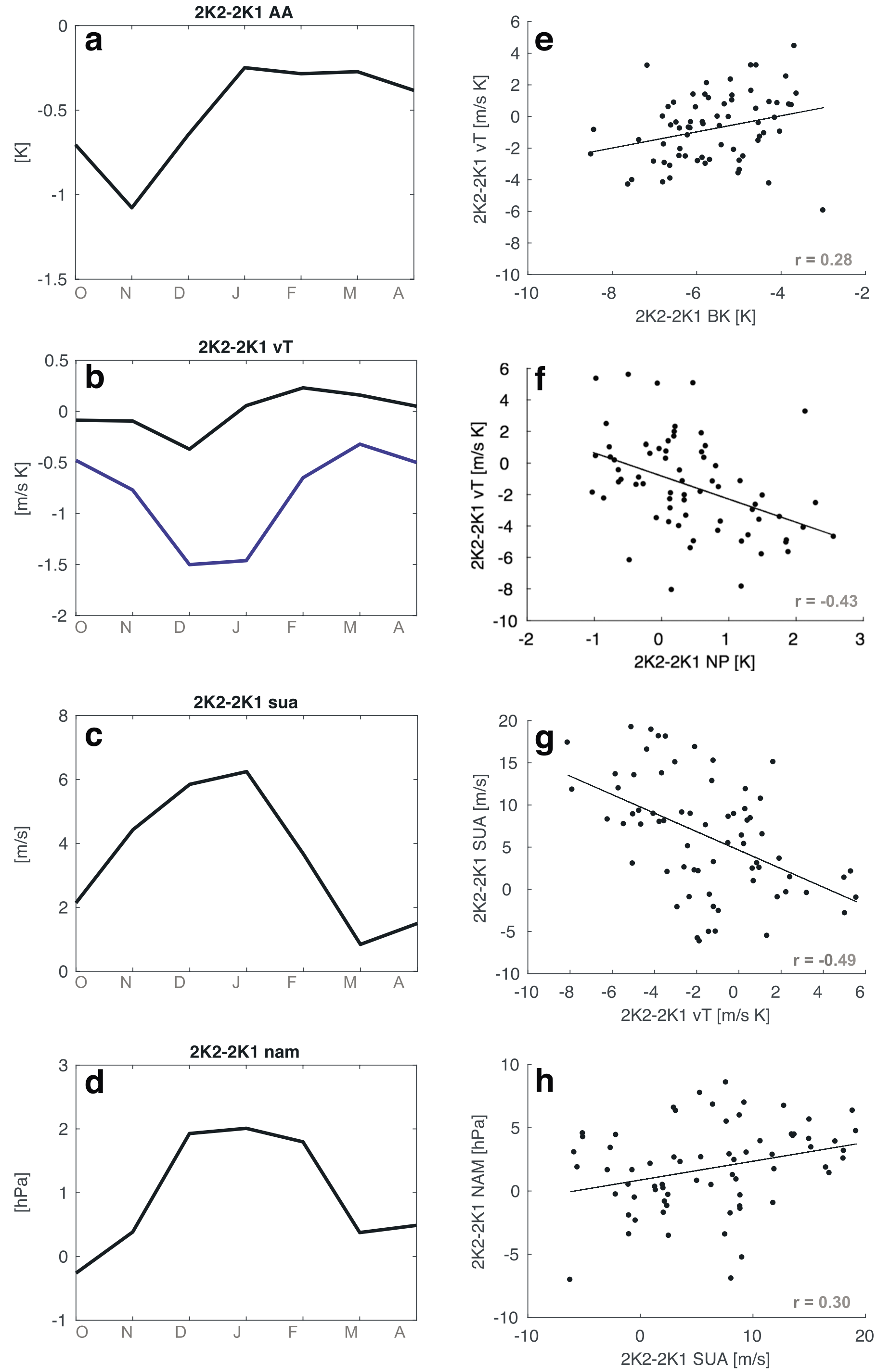

Figure 2. Difference (2K2 − 2K1) in the response for October to April ensemble means of (a) Arctic amplification (850-hPa temperature, 60°–90°N average, K); (b) quasi-stationary meridional eddy heat flux index (hereafter HFI, 45°–85°N average, $m \cdot s^{-1} \cdot K$) at 500 hPa (black) and 100 hPa (blue); (c) zonal mean zonal wind index (hereafter UI, 50°–80°N average, 10 hPa, m/s); and (d) northern annular mode pressure at sea level index (30°–50°N average minus 60°–90°N average, hPa); scatterplots between (e) November BK near-surface temperature (10°–100°E and 70°–80°N average, 850 hPa, K) and HFI (100 hPa, $m \cdot s^{-1} \cdot K$); (f) January North Pacific near-surface temperature (160°–200°E and 40°–50°N average, K) and HFI (100 hPa, $m \cdot s^{-1} \cdot K$); (g) January HFI (100 hPa, $m \cdot s^{-1} \cdot K$) and UI (m/s); and (h) January UI (m/s) and February northern annular mode pressure at sea level index (hPa).

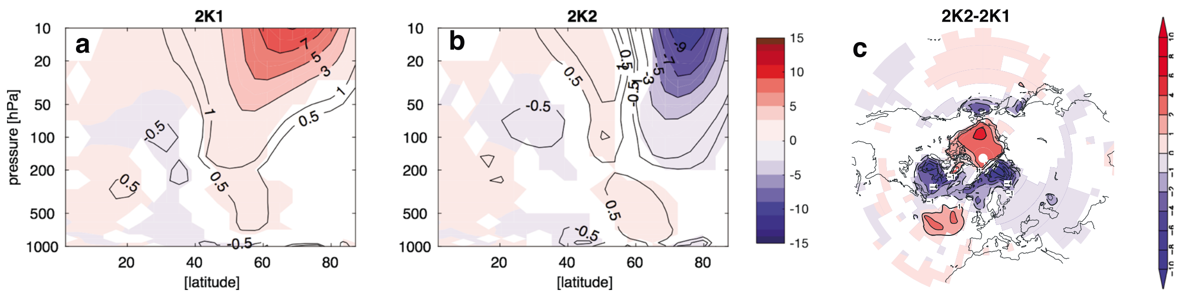

Figure 3. January response of quasi-stationary meridional eddy heat flux (m · s^{-1} · K) to (a) the first and (b) the second 2 K of global warming. Contours: ±0.5, ±1 and then each 2 m · s^{-1} · K. (c) Difference (2K2 − 2K1) in the January near-surface temperature response. Contours: ±1, ±2 and then each 2 K. Colored areas indicate significance with $p < 0.05$.

February suggests that the difference in the atmospheric changes, possibly triggered by AA, is sustained throughout the winter and coupled back to the surface via the stratospheric pathway (Nakamura et al., 2016).

In support of the ensemble mean results, we ask if the relationship between the AA and the atmospheric nonlinearities can also be found across the members. To this end, Figures 2e–2h shows scatterplots composed of the (2K2 − 2K1) nonlinear signatures, by member. The scatterplots show that the variability of the nonlinearity is very high, given the relatively small correlations. However, all the relationships shown in Figures 2e–2h are significant with $p < 0.05$.

Early winter BK sea ice loss has been shown to provide a wave activity source leading to a stratospheric vortex weakening (Hoshi et al., 2017; Nakamura et al., 2016; Sun et al., 2015). Hence, we first examine the relationship between the nonlinearities in the lowermost stratospheric SHF and the near-surface warming in the BK region, in November (Figure 2e). Moreover, the BK region has the largest nonlinearity in the ensemble mean and the same seasonality and sign of AA (not shown). Figure 2e indicates that most of the members with the largest reductions (for instance, 2K2 − 2K1 < −2 m · s^{-1} · K) in the SHF change also have the largest reductions in the BK warming.

The reduction in the BK amplification may not be the only factor driving the change in the stratospheric circulation. Indeed, we found also a significant and stronger relationship between the nonlinearity in the North Pacific near-surface warming (positive nonlinearity in the ensemble mean, Figure 3c) and that in the SHF change (Figure 2f, January). According to Hurwitz et al. (2012), warming of the North Pacific and associated weakening of the Aleutian low is related to a strong stratospheric polar vortex via a reduction of wave activity (hence reduction in meridional heat flux). The relationship in Figure 2f, showing larger heat flux reductions for warmer North Pacific, is consistent with this mechanism and suggests a change between the two periods contributing to the strengthening of the stratospheric vortex in 2K2. Although answering why the North Pacific warms more during the second period is left for a subsequent work, we note that the North Pacific nonlinearity may be traced to the sea ice nonlinearity, via a wind-driven ocean response mechanism, one of the mechanisms responsible for the Pacific decadal oscillation (Newman et al., 2016). Evidence of the difference in the change of the wind driving of the ocean is the negative nonlinearity in the zonal wind response east of Japan (Figure 1f), which implies less cold advection from Siberia, and a reduced deepening of the Aleutian low in the second period (Figure 1i), which is consistent with reduced sea ice loss (Screen et al., 2018).

Within the stratosphere, members with a stronger shift to a westerly change (high positive nonlinearity) show a stronger decrease in the stationary heat flux change (Figure 2g, January). The nonlinearity in the circulation change in the stratosphere is therefore of dynamical origin, given that this relationship is expected by wave-mean flow interaction. Further strengthening of the stratospheric vortex can occur due to increased downward reflection, which is favored when the wave activity flux from the troposphere is reduced (Harnik, 2009). However, testing of this hypothesis in the current study is not possible because of the lack of daily data.

The key role of the stratosphere in providing for persistence and downward impacts of the nonlinear atmospheric circulation changes is also found within the intra member spread through the correlation between the NAM index in February and the stratospheric vortex in January (Figure 2h). The relationship among the

10.1029/2018GL077826

differences in the changes, by members, points to stratosphere-troposphere coupling (Kidston et al., 2015). Members with stronger and positive nonlinearity in the stratospheric changes (strong polar vortex for 2K2) also show a stronger and positive nonlinearity in the NAM index changes.

Nonlinearities in the ensemble mean of near-surface temperature over the tropical oceans are generally not significant or relatively small ($<$1 K, not shown). Large negative nonlinearity in near-surface temperature over the Arctic (Figure 3c, January) point to the regions, which are sea ice free at the beginning of 2K2. In the deep Arctic, the positive difference indicates instead where more sea ice melting takes place during 2K2 compared to 2K1. In midlatitudes, one region of nonlinearity (less than 1 K) is in the North Pacific discussed in the previous paragraph. A larger (~1–2 K) positive difference is found over the North Atlantic Ocean. The Atlantic meridional overturning circulation (AMOC) is known to weaken with global warming and in turn to induce a relative surface cooling of the North Atlantic, because the AMOC acts to warm the North Atlantic Ocean. The positive signature in Figure 3c suggests that there is a reduction of the AMOC decrease for 2K2 compared to 2K1. This difference in the changes is consistent with a decrease in freshwater flux into the North Atlantic for 2K2, as suggested by previously reported sensitivity of the AMOC to sea ice changes (Oudar et al., 2017). Of relevance here, is that the 2K2 intensified warming of the North Atlantic possibly cannot drive the stratosphere vortex strengthening. According to Omrani et al. (2014), warming of the North Atlantic sea surface is related indeed to a stratospheric vortex weakening.

5. Discussion and Conclusions

We have examined aspects of the transient mean climate of the atmospheric circulation response for two consecutive periods of 2 K of global warming by analyzing the grand ensemble (68 members) of experiments performed with the MPI-ESM-LR climate model and forced with the idealized 1% per year increase in atmospheric CO_2 concentration, until $4xCO_2$.

We have found a nonlinear response of the mean atmospheric circulation and North Atlantic-European climate to global warming. The nonlinear signature is manifested as a vertically coherent pattern in zonal mean zonal wind, with stronger winds poleward of 50°N and weaker winds to the south, encompassing the stratosphere and troposphere. Large nonzonal differences between the responses to the 2 K of global warming emerge over the North Atlantic region, where a seesaw PSL change and poleward shifted near-surface zonal winds occur only for 2K2 (the second global warming period of 2 K). At the same time, there is a linear response in the tropical upper troposphere warming, which is known to be an important driver of the Northern Hemisphere extratropical circulation changes (Manzini et al., 2014). The linearity in the tropical upper troposphere warming is to be expected, given that the two periods have the same global warming and the known strong relationship between tropical upper troposphere and global warming.

The nonlinear response in the North Atlantic region can be understood in terms of the competing and contrasting influences driven by the tropical upper troposphere warming and the stratospheric polar vortex change. During 2K1 (the first global warming period of 2 K), the stratospheric polar vortex weakens, thus counteracting, by downward coupling, circulation changes driven by the tropical upper troposphere warming, especially over the North Atlantic-European region. Once the stratospheric response reverses and the stratospheric vortex strengthen, the influences of the stratospheric response and tropical upper troposphere warming no longer counteract but reinforce each other. Therefore, near-surface zonal winds increase in the high-latitude North Atlantic region and the positive phase of the NAM intensifies.

From the analysis carried out so far, limited to monthly mean outputs, a plausible reason for the difference in the stratospheric response between the two periods can be traced to the November reduction in Arctic amplification during the second period. AA is decreased, possibly because there is no longer sea ice in the BK and other marginal Arctic seas during 2K2. Thus, we speculate that the BK wave activity source will no longer change during the second period, while other drivers of wave activity change will continue to evolve. Weaker AA for 2K2 may likely lead to increased warming in the North Pacific, which in turn can lead to a direct reduction of a source of wave activity. It is therefore not clear whether the BK and North Pacific changes are independent and addressing this question is left for future research. Further analysis with daily outputs will also be needed to disentangle the evolution of any other drivers of wave activity changes (including the atmospheric climatological basic state, wave propagation, and wave reflection) and how their net effect can lead to a weaker or stronger stratospheric vortex.

The internal variability of the MPI-ESM-LR grand ensemble is substantial. The response to the first 2 K warming is actually a strengthening of the polar vortex, for ~20% of the members of our ensembles. Likewise, ~30% of the members respond with a weakening during the second 2 K warming. Hence, for both periods the spread in the polar vortex responses is close to that found within the CMIP5 model ensemble (~30% of the models disagreed with the multimodel mean, Manzini et al., 2014). The MPI-ESM-LR grand ensemble therefore appears to be representative of the variety of the CMIP5 stratospheric responses, even if part of the spread in the CMIP5 ensemble is due to intermodel structural differences. Model structural differences include model uncertainties related the atmospheric climatological basic state (Sigmond & Scinocca, 2010). Open research questions are therefore to what extent responses and nonlinearities from models with different atmospheric climatological basic states and associated internal variability will reproduce the current results. Moreover, Arctic sea ice loss is not the only mechanism leading to a stratospheric easterly wind change (Karpechko & Manzini, 2017). Specific questions left for future work include also understanding which of these mechanisms dominate and whether they are additive.

In summary, we have shown that there can be a nonlinear response of the atmospheric circulation response to global warming and we provided evidence that differences in the evolution of the sea ice changes may trigger the nonlinearity of the atmospheric response, which is sustained throughout the winter and coupled back to the surface via the stratospheric pathway. This work, therefore, highlights that determining the atmospheric circulation response to global warming is complex and the transient mean climate needs to be investigated, because of the many contrasting influences and their changing contributions to climate change. To disentangle these questions, research should aim at a better understanding of the multiple connections between the sea ice, ocean, and atmospheric responses. To test the robustness of our single-model results, large ensemble of experiments with more models is needed.

Acknowledgments
We are grateful to Daniela Matei, Jurgen Bader, Marco Giorgetta, Nili Harnik, Sebastian Milinski, Evangelos Tyrlis, and Jin-Song von Storch for discussions and suggestions. E. M. acknowledges support from the MPG MINERVA program and the BMBF project CLIMPRE InterDec (FKZ: 01LP1609A) within the framework of JPI CLIM Belmont-Forum InterDec consortial project. A. Yu. K. is supported by the Academy of Finland (grants 286298 and 294120). Primary data used in this work will be archived by the Max Planck Institute for Meteorology and made available by contacting publications@mpimet.mpg.de prior to publication.

References

Giorgetta, M. A., Jungclaus, J., Reick, C. H., Legutke, S., Bader, J., Böttinger, M., et al. (2013). Climate and carbon cycle changes from 1850 to 2100 in MPI-ESM simulations for the Coupled Model Intercomparison Project phase 5. *Journal of Advances in Modeling Earth Systems*, *5*(3), 572–597. https://doi.org/10.1002/jame.20038

Harnik, N. (2009). Observed stratospheric downward reflection and its relation to upward pulses of wave activity. *Journal of Geophysical Research*, *114*, D08120. https://doi.org/10.1029/2008JD010493

Hoshi, K., Ukita, J., Honda, M., Iwamoto, K., Nakamura, T., Yamazaki, K., et al. (2017). Poleward eddy heat flux anomalies associated with recent Arctic sea ice loss. *Geophysical Research Letters*, *44*, 446–454. https://doi.org/10.1002/2016GL071893

Hurwitz, M. M., Newman, P. A., & Garfinkel, C. I. (2012). On the influence of North Pacific sea surface temperature on the Arctic winter climate. *Journal of Geophyscal Research*, *117*, D19110. https://doi.org/10.1029/2012JD017819

Karpechko, A. Y., & Manzini, E. (2012). Stratospheric influence on tropospheric climate change in the Northern Hemisphere. *Journal of Geophyscal Research*, *117*, D05133. https://doi.org/10.1029/2011JD017036

Karpechko, A. Y., & Manzini, E. (2017). Arctic stratosphere dynamical response to global warming. *Journal of Climate*, *30*(17), 7071–7086. https://doi.org/10.1175/JCLI-D-16-0781.1

Kidston, J., Scaife, A. A., Hardiman, S. C., Mitchell, D. M., Butchart, N., Baldwin, M. P., & Gray, L. J. (2015). Stratospheric influence on tropospheric jet streams, storm tracks and surface weather. *Nature Geoscience*, *8*(6), 433–440. https://doi.org/10.1038/NGEO2424

Kim, B.-M., Son, S.-W., Min, S.-K., Jeong, J.-H., Kim, S.-J., Zhang, X., et al. (2014). Weakening of the stratospheric polar vortex by Arctic sea-ice loss. *Nature Communications*, *5*, 4646. https://doi.org/10.1038/ncomms5646

Manzini, E., Karpechko, A. Y., Anstey, J., Baldwin, M. P., Black, R. X., Cagnazzo, C., et al. (2014). Northern winter climate change: Assessment of uncertainty in CMIP5 projections related to stratosphere-troposphere coupling. *Journal of Geophyscal Research*, *119*, 7979–7998. https://doi.org/10.1002/2013JD021403

McLandress, C., & Shepherd, T. G. (2009). Simulated anthropogenic changes in the Brewer–Dobson circulation, including its extension to high latitudes. *Journal of Climate*, *22*(6), 1516–1540. https://doi.org/10.1175/2008JCLI2679.1

Meraner, K., Mauritsen, T., & Voigt, A. (2013). Robust increase in equilibrium climate sensitivity under global warming. *Geophysical Research Letters*, *40*, 5944–5948. https://doi.org/10.1002/2013GL058118

Nakamura, T., Yamazaki, K., Iwamoto, K., Honda, M., Miyoshi, Y., Ogawa, Y., et al. (2016). The stratospheric pathway for Arctic impacts on midlatitude climate. *Geophysical Research Letters*, *43*, 3494–3501. https://doi.org/10.1002/2016GL068330

Newman, M., Alexander, M. A., Ault, T. R., Cobb, K. M., Deser, C., di Lorenzo, E., et al. (2016). The Pacific decadal oscillation, revisited. *Journal of Climate*, *29*(12), 4399–4427. https://doi.org/10.1175/JCLI-D-15-0508.1

Omrani, N.-E., Keenlyside, N. S., Bader, J., & Manzini, E. (2014). Stratosphere key for wintertime atmospheric response to warm Atlantic decadal conditions. *Climate Dynamics*, *42*(3-4), 649–663. https://doi.org/10.1007/s00382-013-1860-3

Oudar, T., Sanchez-Gomez, E., Chauvin, F., Cattiaux, J., Terray, L., & Cassou1, C. (2017). Respective roles of direct GHG radiative forcing and induced Arctic sea ice loss on the Northern Hemisphere atmospheric circulation. *Climate Dynamics*, *49*(11-12), 3693–3713. https://doi.org/10.1007/s00382-017-3541-0

Scaife, A. A., Spangehl, T., Fereday, D. R., Cubasch, U., Langematz, U., Akiyoshi, H., et al. (2012). Climate change projections and stratosphere–troposphere interaction. *Climate Dynamics*, *38*(9-10), 2089–2097. https://doi.org/10.1007/s00382-011-1080-7

Screen, J. A., Deser, C., Smith, D. M., Zhang, X., Blackport, R., Kushner, P. J., et al. (2018). Consistency and discrepancy in the atmospheric response to Arctic sea-ice loss across climate models. *Nature Geoscience*, *11*(3), 155–163. https://doi.org/10.1038/s41561-018-0059-y

Sigmond, M., & Scinocca, J. F. (2010). The influence of the basic state on the Northern Hemisphere circulation response to climate change. *Journal of Climate*, *23*(6), 1434–1446. https://doi.org/10.1175/2009JCLI3167.1

Sun, L., Deser, C., & Thomas, R. A. (2015). Mechanisms of stratospheric and tropospheric circulation response to projected Arctic Sea ice loss. *Journal of Climate*, *28*(19), 7824–7845. https://doi.org/10.1175/JCLI-D-15-0169.1

Taylor, K. E., Stouffer, R. J., & Meehl, G. A. (2012). An overview of CMIP5 and the experiment design. *Bulletin of the American Meteorological Society*, *93*(4), 485–498. https://doi.org/10.1175/BAMS-D-11-00094.1

Thompson, D. W. J., & Wallace, J. M. (2000). Annular modes in the extratropical circulation. Part I: Month-to-month variability. *Journal of Climate*, *13*(5), 1000–1016. https://doi.org/10.1175/1520-0442(2000)013%3C1000:AMITEC%3E2.0.CO;2

Zappa, G., & Shepherd, T. G. (2017). Storylines of atmospheric circulation change for European regional climate impact assessment. *Journal of Climate*, *30*(16), 6561–6577. https://doi.org/10.1175/%20JCLI-D-16-0807.s1